Hindawi Publishing Corporation
Journal of Nanomaterials
Volume 2014, Article ID 240950, 13 pages
http://dx.doi.org/10.1155/2014/240950

Research Article

Nanocrystallization of the Pharmaceutically Active Agent Genipin by an Emulsion Solvent Evaporation Method

Yuangang Zu, Xinyang Yu, Xiuhua Zhao, Weiguo Wang, and Kunlun Wang

Key Laboratory of Forest Plant Ecology, Northeast Forestry University, Ministry of Education, Harbin, Heilongjiang 150040, China

Correspondence should be addressed to Xiuhua Zhao; xiuhuazhao@nefu.edu.cn

Received 13 March 2014; Accepted 11 June 2014; Published 6 July 2014

Academic Editor: Abdelwahab Omri

To improve the water solubility and dissolution rate, genipin was nanocrystallized by an emulsion solvent evaporation method, followed by freeze-drying. The optimization condition of nanocrystallization process was carried out by single-factor experiment. The effects of five experimental parameters, such as concentration of surfactants the proportion of water to organic phase, homogenate speed and time, homogenization pressure and times, and the proportion of genipin to lyoprotectants on the mean particle size (MPS) of genipin nanoparticles, were investigated. Under the optimum conditions by single-factor experiments, genipin nanoparticles with an MPS of 59.8 nm were obtained. The genipin nanoparticles were characterized by SEM, FTIR, XRD, DSC, solvent residue, drug purity test, dissolution testing, and bioavailability analysis. The analysis results indicated that the chemical structure of genipin nanoparticles was unchanged, but the crystallinity was reduced. The solubility of genipin nanoparticles was 9.05 times of the raw drug. In addition, the residual amounts of chloroform and ethanol were separately less than the ICH limit for class II, and the oral bioavailability of the genipin nanoparticles powder was 7.99 times of raw genipin. According to the results above, genipin nanoparticles show the potential application value of its oral absorption.

1. Introduction

Genipin (Figure 1) is an active compound, derived from iridoid glycosides-geniposidic (GENIPOSIDE) in the fruit of Gardenia. Genipin is also an intestinal metabolite from geniposide, which plays the main role in vivo pharmacological activities [1]. Genipin has been reported to have different effects such as antimicrobial [2], antitumor [3], anti-inflammatory [4], treatment of diabetes [5], hepatoprotective [6], and neurotrophic [7] effects. Genipin may also have a significant effect as an antidepressant through regulating gut microbes [8], energy metabolism, and glycometabolism. In addition, genipin is applied to natural biomaterials as a novel crosslinking agent, with advantage of high biocompatibility and low cell toxicity [9]. Moreover, the spontaneous reaction of colorless genipin with amino acids can form blue pigments which have been widely used in the food industry in East Asia. Further studies showed that the blue pigments have been developed as a new kind of health-enhancing nutritional food for the prevention and treatment of inflammatory diseases because of their anti-inflammatory properties [10].

Thus, the various uses of genipin are increasingly researched. However, the application of genipin in oral administration is restricted as a result of poor aqueous solubility and low dissolution rate. These are the main barriers for the wide use of genipin in pharmaceutical formulations.

Various methods have been used to improve dissolution, aqueous solubility, and bioavailability of poorly soluble drugs. Such as preparation of nanoparticles [11], the use of solubilizer and surfactants [12], and the formation of solid dispersions [13, 14]. Particularly, preparation of nanoparticles shows a bright application prospect due to its simple process and long-term stability [15]. Currently, preparation of nanoparticles mainly includes both bottom-up and top-down techniques [16]. Bottom-up technique is used to control the process of pharmaceutical precipitation and nanocrystallization based on molecule form of drugs, such as precipitation technology, supercritical-fluid technology (rapid expansion of supercritical solution (RESS) [17], gas antisolvent (GAS)), emulsification technology [18], and microemulsification method, while the top-down technique is used to grind pharmaceutical

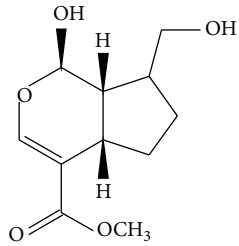

Figure 1: Chemical structure of genipin (MW = 226.23).

powder into nanoparticles through mechanical force, including media milling technique and the high-pressure homogenization technique [19]. However, one technique alone may be somewhat inadequate and the experimental results are unsatisfactory [20]. Zhao and colleague [21] reduced the particle size of genipin by an antisolvent precipitation process. Although that process enhanced the aqueous solubility and dissolution rate of genipin to a certain extent, genipin was just micronized to be an MPS of 1.8 μm. Moreover, Zhang and colleague [22] improved the aqueous solubility and dissolution rate of genipin significantly by genipin/hydroxypropyl-β-cyclodextrin (HP-β-CD) inclusion complex, but the costs of HP-β-CD are relatively high. In view of disadvantages, we combined emulsification technology with high-pressure homogenization technique, which is an emulsion solvent evaporation method. Firstly, an appropriate organic phase should be selected. Particular attention is that the solubility of the raw drug in an organic solvent should be high and the organic phase can be soluble in other organic solvents. Moreover, the organic phase containing drugs and water phase are mixed and then fully emulsified. In the next step, the emulsion is processed through high-pressure homogenization. Furthermore, evaporation helps nanoemulsion to remove organic solvent. Lastly, the processed drugs need to be dried by an appropriate method. This technique has been reported to produce several drugs, such as Poly (lactide-co-glycolide) (PLG) microparticles [23] and 10-hydroxycamptothecin-loaded glycyrrhizic acid-conjugated bovine serum albumin nanoparticles [24].

In this work, genipin was nanocrystallized by an emulsion solvent evaporation method to further improve its dissolution rate and solubility, which to our knowledge has been unused in the previous experiments until now. The effects of diverse experimental parameters on particle size and morphology, such as the concentration of the genipin solution, the concentration of poloxamer 188, the proportion of water to organic phase, homogenate speed and time, homogenization pressure and times [25], and the proportion of genipin to mannitol [26] were separately investigated and optimized. The raw genipin and the optimized genipin nanoparticles were, respectively, characterized by SEM, FTIR, XRD, DSC, high-performance liquid chromatography (HPLC), dissolution test, residual solvent determination [27], and bioavailability tests [28].

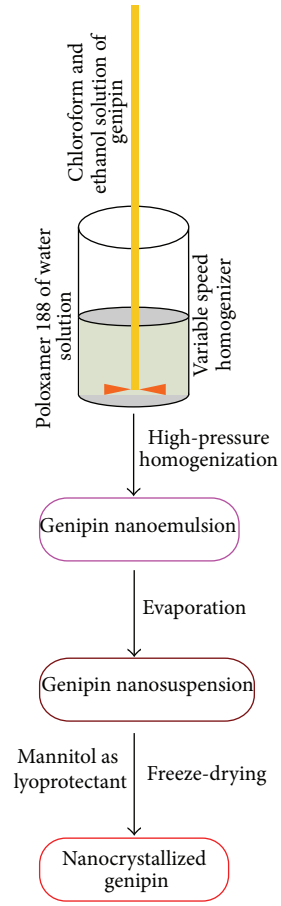

Figure 2: Diagram of the experimental processes to prepare nanocrystallized genipin.

2. Materials and Methods

2.1. Materials. Genipin (purity ≥ 98%) was purchased from Chengdu Conbon Bio-Tech Co., LTD. (Sichuan, China). HPLC-grade methanol, mannitol, and poloxamer 188 were all obtained from Sigma Aldrich (St. Louis, MO, USA). Chloroform (purity > 99.5%), ethanol (purity > 99.5%), and the other reagents were all analytical grades.

2.2. Preparation of Genipin Nanocrystallized. Nanocrystallized genipin was prepared by an emulsion solvent evaporation method. A diagram of the experimental processes to prepare nanocrystallized genipin is shown in Figure 2. Briefly, the process included three main steps: emulsion preparation, solvent evaporation, and lyophilization. A certain amount of raw genipin was completely dissolved in a mixture that consisted of chloroform and ethanol. The solution was added dropwise to deionized water with poloxamer 188, mixing with high-speed homogenizer (FSH-II, Jiangsu, China) and homogenized in nanohomogenize machine (AH-100D, ATS Engineering Inc., Canada), and then the first step was finished after genipin nanoemulsion being obtained. On the second phase, the organic phase was removed by rotary evaporation using a rotary evaporator R201BL (SENCO, Shanghai, China)

Table 1: Factors and levels of the single-factor experiments when one variable factor and others are fixed.

Factor	(A)	(B)	(C)	(D)	(E)	(F)	(G)
Levels	Concentration of poloxamer 188 (‰)	The proportion of water to organic phase (v/v)	Homogenate speed (rpm)	Homogenate time (min)	Homogenization pressure (bar)	Homogenization times	The proportion of genipin to mannitol (m/m)
1	1	9 : 1	5000	1	400	3	1 : 3
2	2	10 : 1	7500	3	600	6	1 : 5
3	3	11 : 1	10000	5	800	9	1 : 7
4	4	12 : 1		7		12	1 : 9
5	5	13 : 1		9			
6		14 : 1		11			
7		15 : 1					
8		16 : 1					
9		17 : 1					
10		18 : 1					

at 50°C and then genipin nanosuspension was obtained. Finally, the nanosuspension was freeze-dried at −50°C for 24 h and mannitol was added in some of the nanosuspension as lyoprotectant. Because lyoprotectant does not take part in chemical reactions, the final step ended with successful preparation of two kinds of nanocrystallized genipin: genipin nanoparticles without mannitol and genipin nanoparticles. Every experiment was repeated at least three times.

2.3. Optimization of the Preparation of Genipin Nanocrystallized

2.3.1. Optimization of the Preparation of Genipin Nanoemulsion. Before optimizing the preparation of genipin nanoemulsion, the proportion of chloroform to ethanol was selected by several trials based on the solubility of raw genipin in the organic phase. The results showed that the solubility of raw genipin was maximal in the mixed solvent of 30% chloroform and 70% ethanol, and the maximal solubility was 180 mg/mL. Moreover, the parameters that had effects on particle size were defined through preliminary experiments. The tests indicated that the parameters include the concentration of poloxamer 188, the proportion of water to organic phase, homogenate speed and time, and homogenization pressure (HP) and times. In this study, single-factor method was used to select each optimal condition.

The concentration of poloxamer 188 was ranged from 0.1% to 0.5%. The proportion of water to organic phase (v/v) was from 10 : 1 to 18 : 1. Homogenate speed was ranged from 5000 to 10000 rpm and its time was set from 1 min to 11 min. HP was set from 400 bar to 800 bar and times were set from 3 to 12 times. All the levels are shown in Table 1.

2.3.2. Optimization of the Preparation of Genipin Nanocrystallization. Lyoprotectant had a significant effect on the MPS in genipin nanocrystallization through preliminary experiments. In the lyophilization step mannitol was added in some of the genipin nanosuspension. The proportion of genipin to mannitol (mass/mass) was ranged from 1 : 1 to 1 : 9, which was defined through preliminary experiments. All the levels are also shown in Table 1.

2.4. Characterization of Genipin Nanocrystallization

2.4.1. Morphology Analysis and Particle Size Analysis. The state of the system after homogenate and HP homogenization emulsification was, respectively, observed by optical microscope (Olympus, BH-2, Germany). Furthermore, the morphology of particles was ascertained by SEM (Quanta 200, FEI). The suitable amount of raw genipin powder was onto the carbon tape on the surface of an aluminum stub directly. The drops from the state of the lyophilized sample dissolving in pure water were dropped on silver paper and then the blow-dried silver paper was installed on aluminum stubs by use of double sided carbon tape. Before analysis, the samples were sputter-coated with gold under an argon atmosphere.

The sample was prepared by dilution in pure water and then the MPS of samples was detected by laser light scattering by a ZetaPlus Analyzer (Brookhaven Instruments, Holtsville, NY, USA). Every measurement was repeated three times.

2.4.2. FTIR Analysis. The chemical components of mannitol, raw genipin, genipin nanoparticles without mannitol, and genipin nanoparticles were detected through FT-IR spectroscopy by use of IRAffinity-1 spectroscope (Shimadzu Corporation, Japan). The samples were diluted with KBr mixing powder at 1% and pressed to self-supporting disks, respectively. The analytical range of the spectra at room temperature was from 4000 to 400 cm^{-1} at the resolution of 2 cm^{-1}.

2.4.3. XRD Analysis. The XRD patterns were used to confirm the crystal forms of raw genipin, genipin nanoparticles without mannitol, and genipin nanoparticles, which were recorded by use of a Cu target tube at 30 mA and 40 kV with an X-ray diffractometer with a rotating anode (Philips, Xpert-Pro, The Netherlands). Then 10 mg samples of genipin

particles were weighed into the sample pool. The other samples were filled to the same depth inside the sample holder by leveling with a spatula. The scanning rate (5°/min) was constant for all XRD analysis. The scanning ranged from 5° to 60° with a step size of 0.02°.

2.4.4. DSC Analysis. DSC (TA instruments, model DSC 204) was conducted for raw genipin, genipin nanoparticles without mannitol, and genipin nanoparticles. Five milligrams of the sample was weighed into the sample pool to be scanned from 20 to 200°C at a rate of 10°C/min.

2.4.5. Gas Chromatography (GC) Analysis. The residual amounts of chloroform and ethanol in the genipin nanoparticles were determined by an Agilent 7890A gas chromatograph (Agilent Technologies, Palo Alto, CA, USA) with a HP-5 5% phenyl methyl siloxane capillary column (30.0 m × 320 μm × 0.25 μm, nominal) and equipped with a G1540N-210 FID detector. Peaks areas were used for getting quantitative data. The conditions of gas chromatography (GC) analysis of chloroform were as follows: the oven temperature was initially maintained at 40°C for 8 min and then ramped at a rate of 4°C/min to 240°C and held for 6 min. The injector and the detector temperatures were both set at 280°C. Nitrogen at a purity of 99.999% was used as carrier gas at a flow rate of 30 mL·min^{-1}. Then 10 mg of genipin nanoparticles were dissolved by 1 mL methanol and centrifuged at 8000 rpm for 5 min, and 1 μL samples were manually injected in split mode, with a split ratio of 20 : 1. The flow rate of hydrogen gas was 30 and that of air was 400 mL·min^{-1}, respectively. The conditions of GC analysis of ethanol were as follows: the oven temperature was initially maintained at 40°C for 8 min and then ramped at a rate of 40°C/min to 240°C and held for 10 min. The injector temperature was set at 200°C and the detector was 280°C, respectively. Nitrogen with a purity of 99.999% was used as carrier gas at a flow rate of 25 mL·min^{-1}. Then 10 mg of genipin nanoparticles were dissolved by 1 mL deionized water and centrifuged at 8000 rpm for 5 min. 1 μL samples were injected manually in split mode, with a split ratio 2 : 1. The hydrogen gas and air flow rates were 30 and 400 mL·min^{-1}, respectively.

2.4.6. HPLC Conditions. A Waters chromatograph (Waters Corp, USA) HPLC was used for HPLC. The chromatographic column was a Diamonsil C_{18} reverse-phase column (250 mm × 4.6 mm, 5 μm; China). The mobile phase consisted of 50 : 50 v/v mixtures of methanol and water. The column was maintained at room temperature. The injection volume was 10 μL and the flow rate was 1.0 mL·min^{-1}. The effluent was set at 238 nm.

2.4.7. Drug Purity Test. The drug purity tests of raw genipin, genipin nanoparticles without mannitol, and genipin nanoparticles were investigated by HPLC. 15 mg of raw genipin, genipin nanoparticles without mannitol, and genipin nanoparticles was dissolved in 10 mL ethanol solution, respectively. The drug solution was shaken for 60 min by ultrasonic agitation at 20°C. Then the samples were diluted 10 times with ethanol solution. The drug solution was centrifuged at 10000 rpm for 10 min. Then 10 μL of the supernatant was directly injected into the HPLC system. The analysis conditions were the same as described in Section 2.4.6. The experiment was repeated in triplicate.

2.4.8. Dissolution Study. The dissolution study of raw genipin, genipin nanoparticles without mannitol, and genipin nanoparticles was performed by HPLC. The paddle speed was set at 100 rpm at a solution temperature of 37.0 ± 0.5°C. Artificial gastric juice was made by mixture of 5 mL 37% hydrochloric acid and 1000 mL pure water, which was used as the dissolution medium [29]. Raw genipin (110 mg), genipin nanoparticles without mannitol (containing 110 mg genipin), and genipin nanoparticles (containing 110 mg genipin) were separately added to 100 mL of dissolution medium. Samples (2 mL) were withdrawn at 0.1, 0.5, 1, 2, 3.5, 5, 10, 20, 30, 45, and 60 min, filtered by the use of a 0.22 μm filter, and then the same volume of dissolution medium was supplemented. The filtrate samples were directly injected into the HPLC system and then the genipin concentration was assayed. The analysis conditions were the same as described in Section 2.4.6. The experiment was repeated three times.

2.5. Bioavailability Study

2.5.1. Animals and Treatment. Six male Sprague-Dawley rats, weighing 200–250 g, were used in this study. Rats were randomly divided into two groups, each with three animals. Prior to all experiments, animals were fasted overnight and water was given ad libitum.

30 mg raw genipin and genipin nanoparticles were dispersed in 3 mL deionized water, respectively. In this study, two groups of 3 male rats were carried out by the oral route (60 mg/kg by gavage due to high water solubility). Blood samples were taken from the orbital venous sinus by puncture [30] and then were immediately collected into heparinized tubes in the following time points: 0, 5, 15, 30, 45, 75, 105, 165, 225, 345, and 585 min after oral administration. The samples were immediately centrifuged at 3000 rpm for 5 min and plasma was separated from sedimented cells with a pipet. Samples were stored deep frozen at −40°C until additional extraction and analysis [31–33].

2.5.2. Preparation of Plasma Sample. Frozen samples after being thawed at room temperature were treated as follows. Each 200 μL of plasma sample was combined with 1000 μL of ethanol and then vortexed for 3 min. After centrifugation at 3000 rpm for 10 min, 800 μL of supernatant was transferred and the residue, described above, was mixed with 800 μL of ethanol for another extraction procedure. Eventually, both of the supernatants were combined and evaporated at 40°C by use of a gentle stream of nitrogen. The dry residue was then reconstituted in 800 μL ethanol, vortexed for 1 min and centrifuged at 12000 rpm for 10 min. The supernatant was placed in the HPLC autosampler, where 10 μL is injected for HPLC analysis. The analysis conditions were the same as

described in Section 2.4.6. The oral bioavailability of genipin nanoparticles was calculated by comparing the corresponding values of AUC from the two groups.

$F = (AUC_{ba}/AUC_{rb}) * 100\%$, where AUC_{ba} is the area under the plasma concentration-time curve of genipin nanoparticles and AUC_{rb} is the area under the plasma concentration-time curve of raw genipin.

3. Results and Discussion

3.1. Optimization Study. The optimal conditions were chosen by use of a single-factor test. When determining one of the factors, the other factors acted as fixed parameters. During preliminary experiments, the following factors having effects on particle size were determined: concentration of poloxamer 188, the concentration of the genipin solution, the proportion of water to organic phase, homogenate speed and time, homogenization pressure and times, and the proportion of genipin to mannitol.

3.1.1. Effect of the Surfactants. The first factor was concentration of poloxamer 188 [34]. Figure 3(a) showed the effects of the concentration of surfactant on MPS. Poloxamer 188, a high macromolecule nonionic surfactant was selected as the surfactant during emulsification. When the amount of poloxamer 188 increased from 1 to 0.2%, the MPS of genipin nanoemulsion decreased significantly. On the contrary, the MPS increased when the volume of poloxamer 188 increased to 0.3%. The MPS of genipin nanoemulsion obviously decreased from 368.6 nm to 264.8 nm as the volume ratio of poloxamer 188 ranged from 3 to 0.5%. Therefore, the optimum volume ratio of poloxamer 188 is 0.5%.

3.1.2. The Effect of the Proportion of Water to Organic Phase. The volume ratio of water to organic phase was the second factor to be considered. The ratios were examined to be within the range of 9 : 1 to 18 : 1. From Figure 3(b), it can be clearly seen that with the increasing volume ratio of water to organic phase, the MPS of genipin nanoemulsion fluctuated increasingly between 366.2 and 1808.8 nm. Finally, the ratio of 10 : 1 was selected as the optimal proportion of water to organic phase to use in subsequent tests after the water and organic phase were tested to form a stable emulsion system.

3.1.3. The Effect of Homogenate Speed and Time. From Figure 3(c), homogenization speeds were tested to be in the range of 5000–10,000 rpm and homogenization time of 1–11 minutes. The already established optimal poloxamer 188 concentration (0.5%) and ratio volume of water to organic phase (10 : 1) were used. At a speed of 5000 rpm, the resultant particle size was 1024.5 nm after the first minute and this decreased sharply to 689.5 nm after 3 minutes. Over the next 5–11 minutes, the particle size gradually decreased to 295.1 nm. Thus, it was clear that it was useful to homogenize at low speed for a long period. At a speed of 7500 rpm, particle size fluctuated between 513.2 and 731.7 nm. At the 3rd minute, the size of the particle had increased to 701.8 nm. However, the particle size decreased to 599.6 nm after 5 minutes. During the 7–11 minutes, the size of the particle gradually became decreased. Therefore, the changes in particle size were found to be unstable at 7500 rpm. Furthermore, the length of time had no significant effect on the size of particles. At the first minute of 10,000 rpm, the particle size was 288.6 nm, which was smaller than that at any time at this period. It is clear that longer time was not helpful because it negatively influenced the goal of reaching a smaller size of particles. Finally, the particle size (59.8 nm) at the speed of 10000 rpm for a duration of 1 minute was the smallest of all, which was chosen as being optimal.

3.1.4. The Effect of Homogenization Pressure and Times. The HP homogenization can make sure that smaller and more uniform droplets are obtained. A sample was prepared under the optimal conditions as described; a poloxamer 188 concentration of 0.5%, a ratio volume of 10 : 1 of water to organic phase, and a homogenization speed of 10000 rpm for 1 minute to examine the influence of homogenization pressures and the times at each pressure on particle size; see Figure 3(d). Homogenization pressures were tested to be in the range of 400–800 bar and homogenization times between 3 and 12. At a pressure of 400 bar, the particle size decreased to 21.2 nm after 6 times, but it became larger during the 9th and 12th times. So longer time was not helpful for obtaining smaller droplets. At a pressure of 600 bar, a good emulsified state was examined after 9 homogenizations, at which point the particle size was 6.1 nm. After 12 homogenizations, the particle sizes were 70.7 nm. At a pressure of 800 bar, the particle sizes were larger than the ones at a pressure of 600 bar. Similarly, a good state of emulsification at this pressure also occurred after 6 homogenizations. In conclusion, the smaller and more uniform nanoemulsion could be obtained at the moderate homogenization pressure and times. Therefore, a pressure of 600 bar and 9 homogenizations were selected as optimal, and the optimum genipin nanoemulsion with an MPS of 6.1 nm was obtained.

The state of the system after homogenate and HP homogenization emulsification was, respectively, observed by optical microscope with many small oil-in-water droplets, as shown in Figure 4. Moreover, abundant droplets dispersed in the solvent were seen under magnification of 400x times (Figure 4(a)) and 1000x times (Figure 4(b)). The emulsions observed were in good condition. The steps were completed as soon as possible, because these emulsions were unstable and phase separation would happen within a few minutes after stopping the homogenization procedure because of intense drop coalescence.

3.1.5. The Effect of the Proportion of Genipin to Mannitol. Lyoprotectants play an active role in protecting drug nanoparticles from denaturation, and mannitol is widely used as a lyoprotectant in freeze-dried process. A sample was prepared under the optimal conditions as described after the freeze-dried process and then a certain amount of genipin nanoparticles was completely dissolved in water to test the effects of the proportion of genipin to mannitol from 1 : 1 to 1 : 9 on MPS. From Figure 3(e), particle size visibly tended to

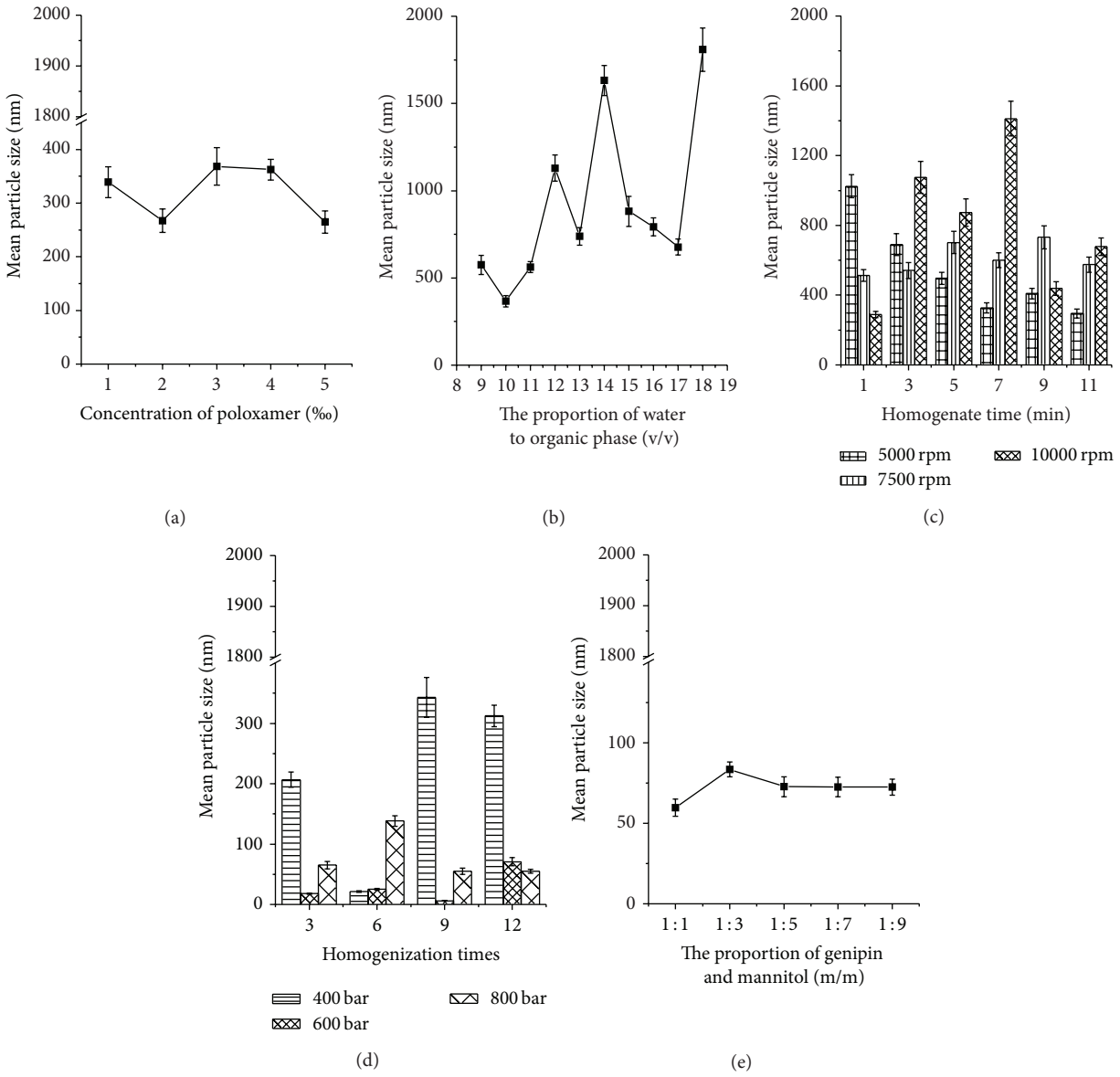

Figure 3: The effect of each parameter on the MPS of nanocrystallized genipin. (a) Concentration of poloxamer; (b) the proportion of water to organic phase; (c) homogenate speed and time; (d) homogenization pressure (HP) and times; (e) the proportion of genipin to mannitol.

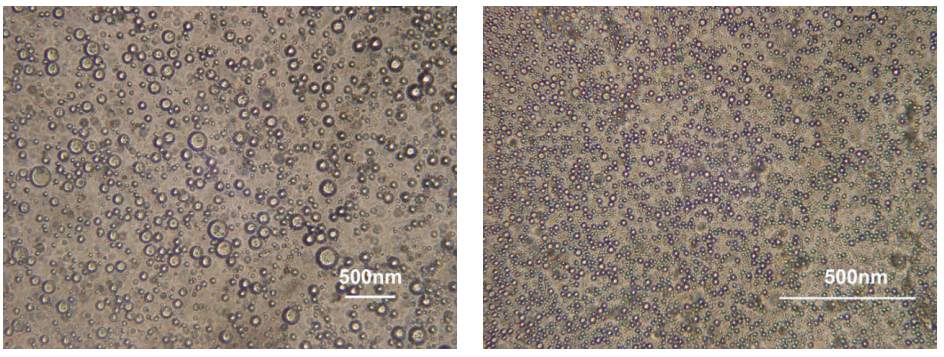

(a) (b)

Figure 4: The state of the system after homogenization observed by optical microscope: (a) 10 × 40 magnification; (b) 10 × 100 magnification.

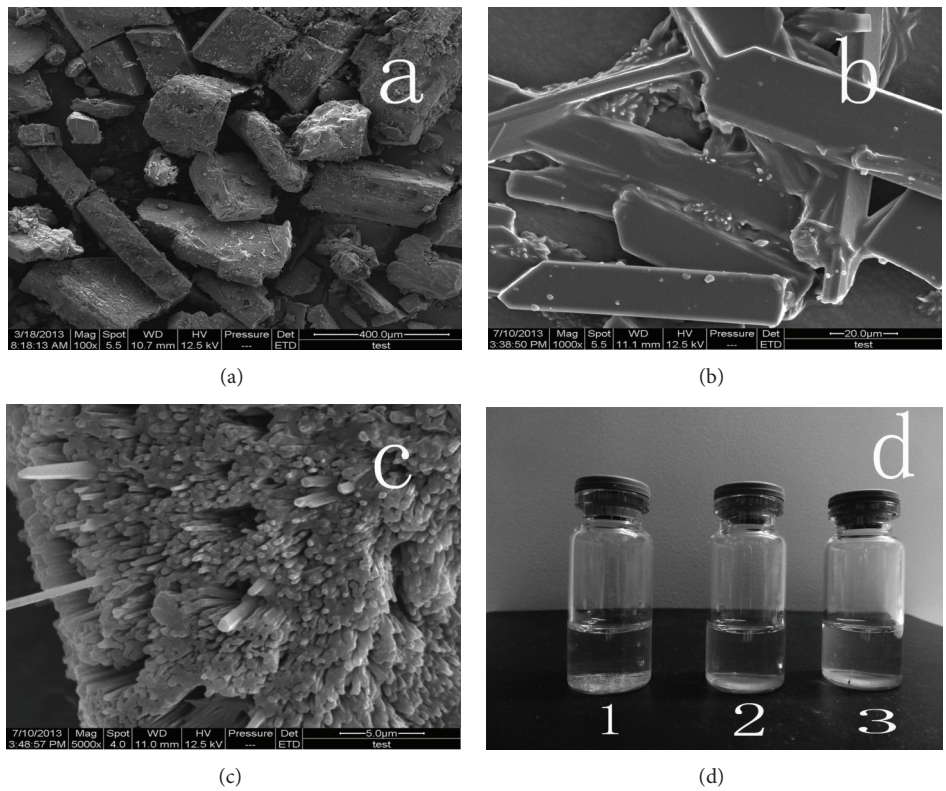

(a) (b) (c) (d)

Figure 5: Morphology of samples observed by SEM: (a) raw genipin; (b) genipin nanoparticles without mannitol; (c) genipin nanoparticles; (d) photograph of the aqueous dispersion of raw genipin (left), genipin nanoparticles without mannitol (middle), and genipin nanoparticles (right).

increase in the ratio range of 1 : 1 to 1 : 3. However, there was a gradual stabilization state at ratios from 1 : 5 to 1 : 9. In view of the particle size, the ratio of 1 : 1 was selected as the optimal proportion of genipin to mannitol to use during the freeze-dried process.

According to the results of single-factor experiments above, the optimal conditions were as follows: 0.5% poloxamer 188, volume ratio of water to organic phase of 10/1, 9 homogenizations at a speed of 10000 rpm for 1 minute each at a pressure of 600 bar, and proportion of genipin to mannitol of 1/1. The subsequent characteristics of the optimum sample were obtained under these conditions.

3.2. Characterization of Nanocrystallized Genipin

3.2.1. Morphology and Particle Diameter of Genipin. The morphology of the samples is shown in Figure 5. The raw genipin appeared as irregular blocks, with a mean particle size of 180 μm in Figure 5(a). Figure 5(b) shows that the particles of genipin nanoparticles without mannitol were nearly regularly stripe. However, genipin nanoparticles were nearly spherical or aciculiform and had a smaller particle size than that without mannitol, as can be seen in Figure 5(c). The MPS in genipin nanoparticles was also far less than 1.8 μm [21]. Figure 6 is the normal distribution curve of genipin nanoemulsion, genipin nanosuspension, the aqueous dispersion of genipin nanoparticles without mannitol, and genipin nanoparticles under optimum condition at one time. Their MPS are 6.1 nm, 47.4 nm, 279.9 nm, and 59.8 nm, respectively. The reason for increasing MPS of genipin nanoparticles without mannitol could be for reunion of particles during freeze-dried process without lyoprotectants. The aqueous dispersion of raw genipin, genipin nanoparticles without mannitol, and genipin nanoparticles are shown in Figure 5(d). In this photograph, it can be seen that raw genipin could not be completely dissolved in the deionized water. Unlike raw genipin, both freeze-dried powder could disperse well in solution, with a transparent opalescence and uniform state [35, 36].

3.2.2. FTIR Analysis. The FTIR spectra of raw genipin, genipin nanoparticles without mannitol, and genipin nanoparticles were taken to obtain the information on the change of chemical structure after nanocrystallization. As presented in Figure 7, raw genipin and genipin nanoparticles without mannitol show the same FTIR spectrum, which demonstrated that there were no differences in the chemical structure. The assignments of the bands were as follows: 3400 cm^{-1} (associate O–H stretching vibration), 3236.99 cm^{-1} (C=C–H stretching vibration), 1685.26 cm^{-1} (C=O stretching vibration of the ester), and 1618.49 cm^{-1} (C=C stretching vibration of the benzene ring). The

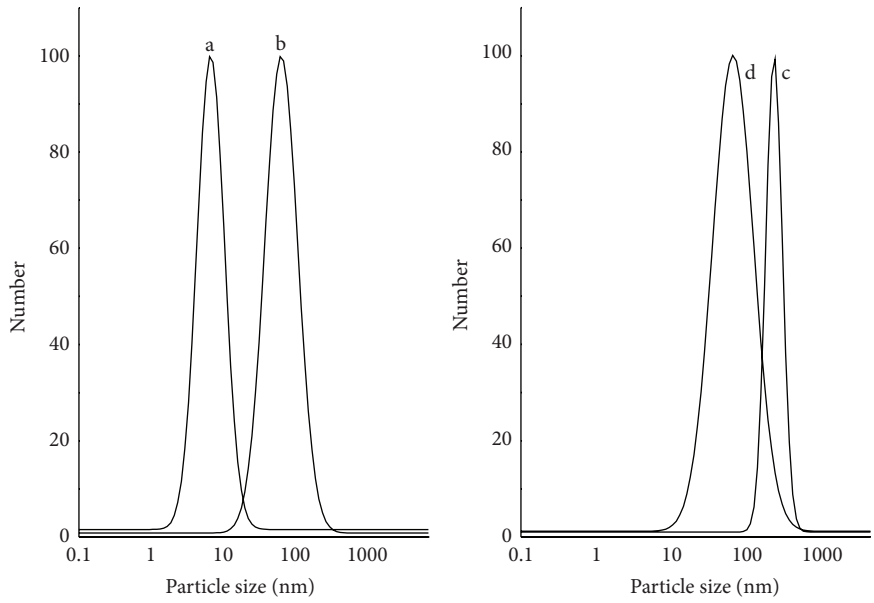

Figure 6: Normal distribution curve of samples: (a) genipin nanoemulsion under optimum condition, (b) genipin nanosuspension under optimum condition, and (c) genipin nanoparticles without mannitol.

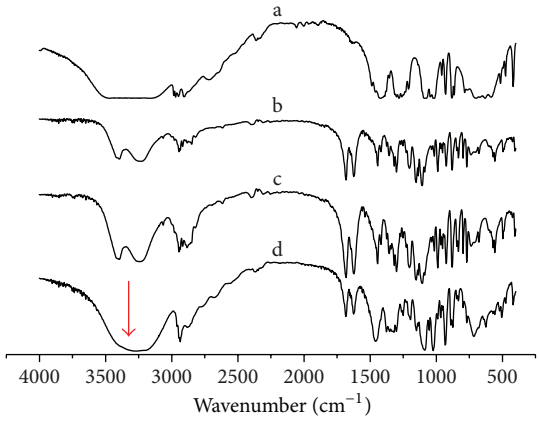

Figure 7: FTIR spectra of mannitol, raw genipin, and genipin nanoparticles. (a) Mannitol, (b) raw genipin, (c) genipin nanoparticles without mannitol, (d) genipin nanoparticles.

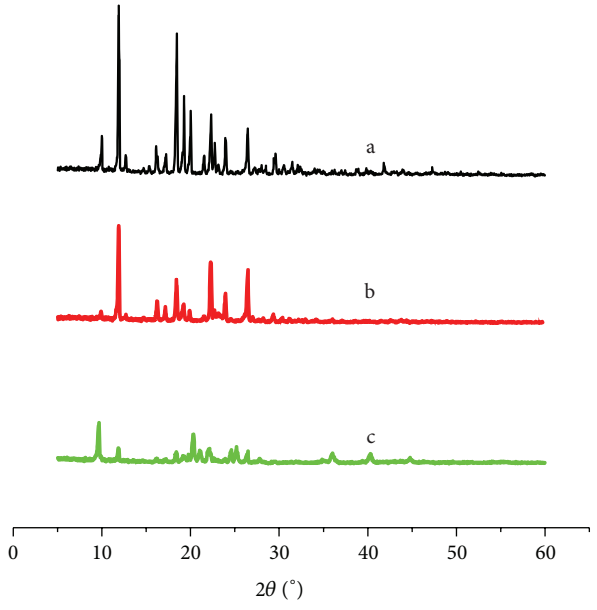

Figure 8: XRD patterns of raw genipin and genipin nanoparticles. (a) Raw genipin, (b) genipin nanoparticles without mannitol, (c) genipin nanoparticles.

spectrum of raw genipin and genipin nanoparticles has some differences at 3400 cm^{-1}, which could be caused by mannitol.

3.2.3. X-Ray Diffraction Studies (XRD). X-ray diffraction was performed to further investigate the occurrence of possible structural changes on the crystalline structure of particles. The XRD analysis of samples containing raw genipin, genipin nanoparticles without mannitol, and genipin nanoparticles is shown in Figure 8. It can be seen that many diffraction peaks could be observed in the XRD curve of raw genipin due to it being highly crystallized. However, both genipin nanoparticles without mannitol and genipin nanoparticles showed only several weak peaks, especially genipin nanoparticles. Less diffraction peaks were attributed to reduce particle crystallinity or a smaller particle size. Furthermore, the genipin nanoparticles might be present in the nearly desired amorphous form. A Less crystalline drug solid is easier to be dissolved than a crystalline solid [37]. As a result, genipin nanoparticles had a higher dissolution rate than raw genipin.

3.2.4. DSC Analysis. The DSC curves of samples are shown in Figure 9, which were used to further confirm the result of

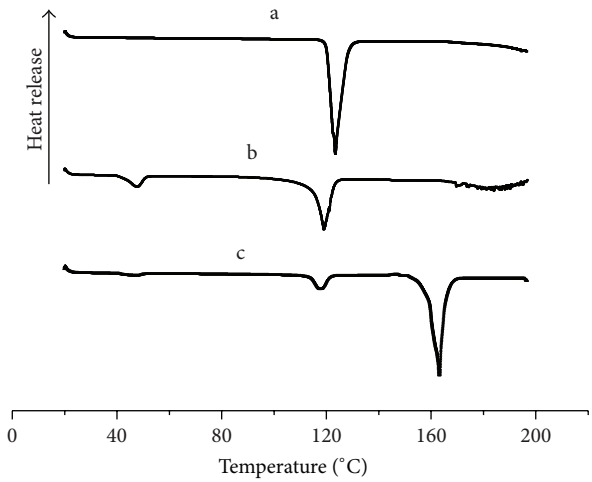

Figure 9: DSC curves of raw genipin and genipin nanoparticles. (a) Raw genipin, (b) genipin nanoparticles without mannitol, (c) genipin nanoparticles.

XRD. The curve of raw genipin showed an endothermic peak at 123.5°C. However, genipin nanoparticles without mannitol showed an endothermic melting peak at 119.0°C and there was an endothermic melting peak at about 117.7°C in the curve of genipin nanoparticles. There was also a peak at about 164.8°C in the curve of genipin nanoparticles and it should be manifested by mannitol. The results indicated that the melting point of genipin nanoparticles without mannitol and genipin nanoparticles had decreased by 4.5°C and 5.8°C, respectively. This evidence confirmed that both genipin nanoparticles without mannitol and genipin nanoparticles had lower crystallinity, in accordance with the XRD results. Genipin nanoparticles, especially, have better dissolution and bioavailability than that without mannitol.

3.2.5. Residual Solvent Content Analysis. The potential risk of solvent residues is also a concern in pharmaceutical products. In this study, genipin nanoparticles were prepared by an emulsion solvent evaporation method using the International Conference on Harmonization (ICH) class II solvent ethanol and chloroform with low toxicity. Figure 10 shows the results of ethanol and chloroform residues using GC. From the chromatograms of the ethanol standard solution (Figure 10(a)), in which ethanol eluted at 2.867 min, a regression equation between peak area (y) and ethanol concentration (x) can be fitted as $y = 371.94x+91.803$ ($R^2 = 0.9997$). According to the regression equation, the residual ethanol content in genipin nanoparticles was 0.05318%. The ICH limit for ethanol in class II solvents is 5000 ppm or 0.5%; therefore, the genipin nanoparticles fully met the ICH requirements and were suitable for pharmaceutical use.

From the chromatograms of the chloroform standard solution (Figure 10(c)), in which the retention time of chloroform was 4.422 min, a regression equation between peak area (y) and chloroform concentration (x) can be fitted as $y = 97967x - 127.34$ ($R^2 = 0.9998$). According to the regression equation, the residual chloroform content in genipin nanoparticles was 0.003883%. Since the ICH limit for chloroform in class II solvents is 60 ppm or 0.006%, the genipin nanoparticles met the ICH requirements and were suitable for pharmaceutical use.

3.2.6. Comparison of Drug Appearance and Purity. Figure 11 shows photographs of the appearance of raw genipin and genipin nanoparticles. Figure 11(a) shows the raw genipin powder, which is a weak yellow needle crystal. Figure 11(b) shows the powder of genipin nanoparticles, which is a fine white flocculent powder. This fact suggests that the appearance of the genipin nanoparticles after the nanocrystallization process have changed from weak yellow needle crystals into a fine white flocculent powder. In addition, analyzing the purity by HPLC showed that the genipin nanoparticles were purified to 38.4%.

3.2.7. Dissolution Results. The dissolution profiles of raw genipin, genipin nanoparticles without mannitol, and genipin nanoparticles are shown in Figure 12. Both genipin nanoparticles without mannitol and genipin nanoparticles showed a more rapid dissolution rate and solubility than raw genipin, especially genipin nanoparticles. The maximum solubility (approximately 39.73 mg·mL^{-1}) was observed in genipin nanoparticles with an MPS of 59.8 nm at 360 min. The maximum solubility of genipin nanoparticles without mannitol was 15.90 mg·mL^{-1} during the same period. However, the maximum solubility of raw genipin was only 4.39 mg·mL^{-1}. At the beginning, 19.1%, 90.6%, and 93.4% of the drugs were dissolved from the raw genipin, genipin nanoparticles without mannitol, and genipin nanoparticles, respectively. Both genipin nanoparticles reached to their maximum solubility at the 2nd minute, which was 92.6% (genipin nanoparticles without mannitol) and 97.2% (genipin nanoparticles), respectively. However, only 56.1% of the raw genipin dissolved during the same period and the raw genipin reached its maximum solubility after 60 minutes. Thus, the dissolution rate of genipin nanoparticles without mannitol and genipin nanoparticles was 1.65 and 1.73 times of the raw drug at the 2nd minute, respectively. In accordance with Noyes-Whitney equation [38], the drug dissolution rate is linear relationship to the surface area exposed to the dissolution medium. The increased dissolution rate and solubility of genipin nanoparticles could be mainly attributed to the great reduction in particle size due to a greater surface area. Therefore, the less crystalline drugs in smaller size can exert their bioactivity efficiently because of their higher dissolution rate and solubility than the crystals.

3.3. Bioavailability Analysis. The result of bioavailability is shown in Figure 13. It can be seen that the concentration in rat plasma of genipin nanoparticles powder group was always higher than that of the raw genipin group. The concentration in rat plasma of the genipin nanoparticles powder and the raw genipin group reached the maximum of 67.71 μg/mL and 2.67 μg/mL after 45 min and 225 min of taking drugs, respectively. Thus, Particle size reduction can help to improve

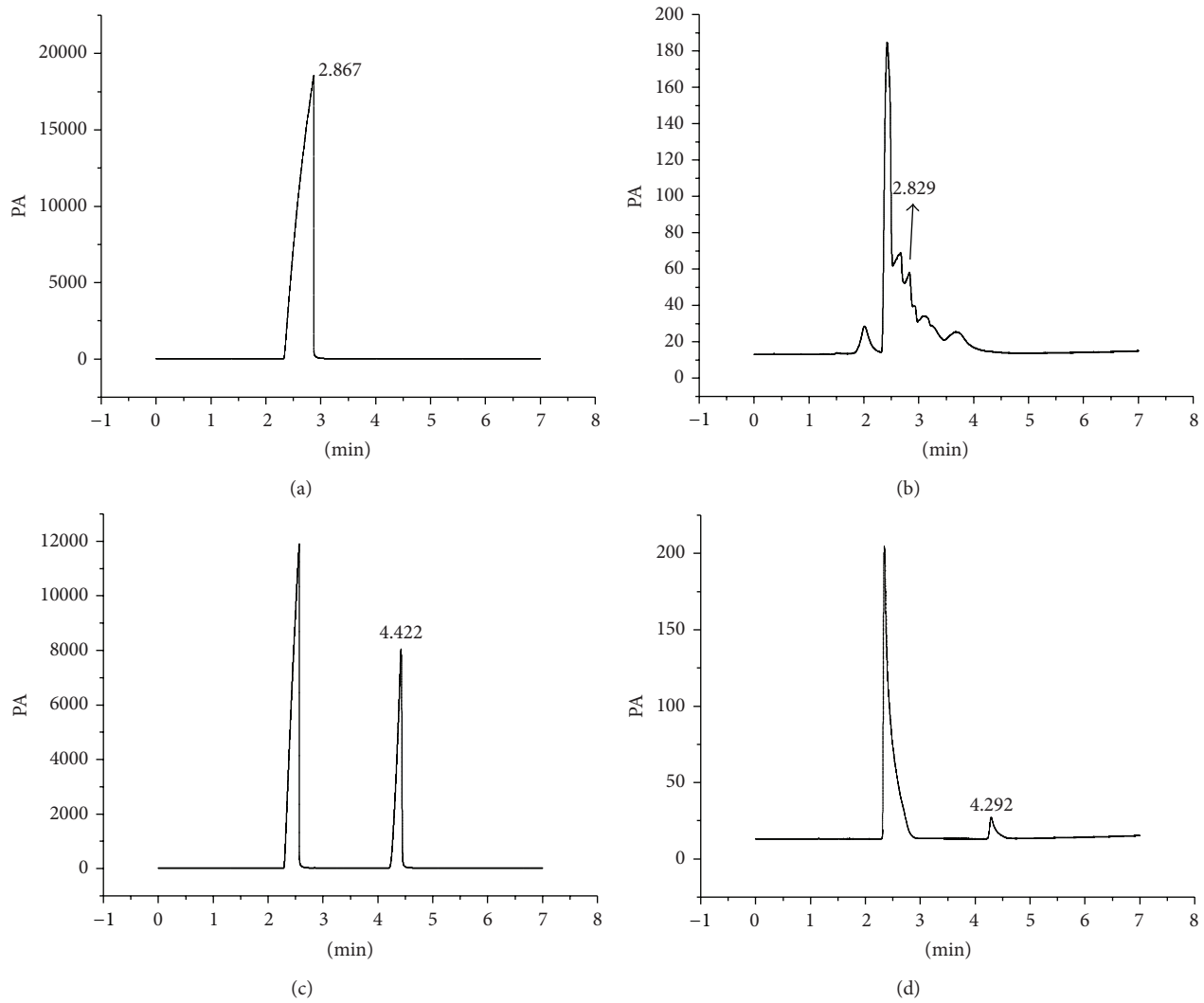

Figure 10: Gas chromatograms of (a) ethanol standard solution, (b) genipin nanoparticles, (c) chloroform standard solution, and (d) genipin nanoparticles.

Figure 11: Photographs of (a) raw genipin and (b) genipin nanoparticles.

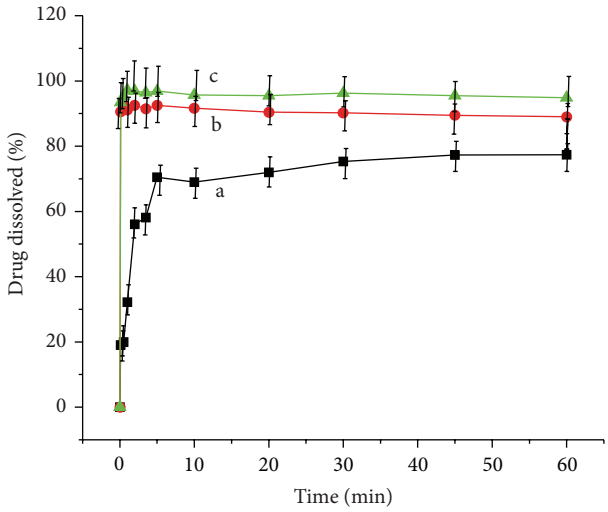

FIGURE 12: Dissolution profiles of raw genipin and genipin nanoparticles: (a) raw genipin, (b) genipin nanoparticles without mannitol, (c) genipin nanoparticles.

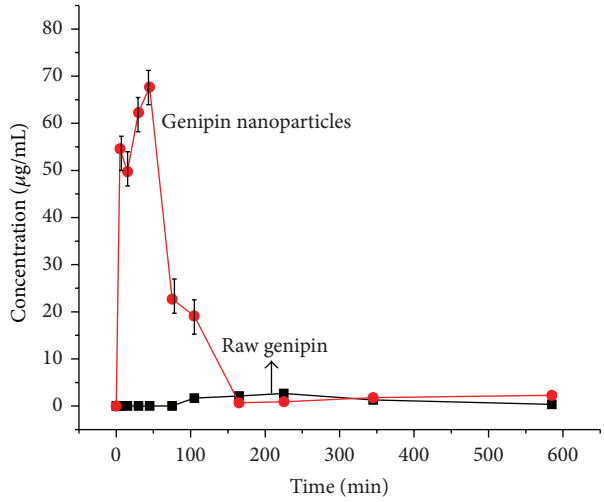

FIGURE 13: Concentration versus time curves of raw genipin and genipin nanoparticles: (a) raw genipin and (b) genipin nanoparticles after drug administration in rats.

the efficiency of genipin absorption. The oral relative bioavailability of genipin nanoparticles powder was calculated by comparing the corresponding AUC values of the two groups, and the results demonstrated that oral administration of genipin nanoparticles led to 799% increase in bioavailability. The significant enhancement of oral bioavailability was also in accordance with the result of the dissolution test and other characterization tests.

4. Conclusions

In this study, genipin nanoparticles were successfully prepared using an emulsion solvent evaporation method, followed by freeze-drying. In this process, poloxamer 188 and mannitol were used as surfactant and lyoprotectant to prevent aggregation from particle growth. The optimal conditions are as follows: 0.5% poloxamer 188, volume ratio of water to organic phase of 10/1, 6 homogenizations at a speed of 10000 rpm for 1 minute each at a pressure of 600 bar, and proportion of genipin to mannitol of 1/1.

Under the optimal conditions, the optimal genipin nanoparticles were obtained with MPS of 59.8 nm. Furthermore, the FTIR analyses demonstrated that genipin nanoparticles had the same chemical structure as raw drug after the emulsion solvent evaporation process. The analysis results of XRD and DSC indicated that the prepared genipin nanoparticles were less crystalline. The residual amount of ethanol and chloroform was 0.05318% and 0.003883%, respectively, which was less than the ICH limit for class II. In addition, the solubility of genipin nanoparticles was 9.05 times of the raw drug. Furthermore, the oral bioavailability of the genipin nanoparticles powder was 7.99 times of raw genipin. In view of pharmacoeconomics, the genipin nanoparticles prepared by an emulsion solvent evaporation method are an inexpensive and efficient oral administration to patients.

Conflict of Interests

The authors declare that there is no conflict of interests regarding the publication of this paper.

Acknowledgments

The authors are grateful for the precious comments and careful corrections made by the anonymous reviewers. The authors would also like to acknowledge the financial support from the National Key Technology R&D Program (2012BAD21B0501) and the National Natural Science Foundation of China (no. 21203018).

References

[1] R. A. A. Muzzarelli, "Genipin-crosslinked chitosan hydrogels as biomedical and pharmaceutical aids," *Carbohydrate Polymers*, vol. 77, no. 1, pp. 1–9, 2009.

[2] B.-S. Liu and T.-B. Huang, "Nanocomposites of genipin-crosslinked chitosan/silver nanoparticles—structural reinforcement and antimicrobial properties," *Macromolecular Bioscience*, vol. 8, no. 10, pp. 932–941, 2008.

[3] S. H. Moon, H. J. Choi, S. J. Lee et al., "Genipin derivative having anti hepatitis B virus activity," Google Patents, 2000.

[4] H.-J. Koo, Y. S. Song, H.-J. Kim et al., "Antiinflammatory effects of genipin, an active principle of gardenia," *European Journal of Pharmacology*, vol. 495, no. 2-3, pp. 201–208, 2004.

[5] C. Zhang, L. E. Parton, C. P. Ye et al., "Genipin inhibits UCP2-mediated proton leak and acutely reverses obesity- and high glucose-induced β cell dysfunction in isolated pancreatic islets," *Cell Metabolism*, vol. 3, no. 6, pp. 417–427, 2006.

[6] M. Yamamoto, N. Miura, N. Ohtake et al., "Genipin, a metabolite derived from the herbal medicine Inchin-ko-to, and suppression of Fas-induced lethal liver apoptosis in mice," *Gastroenterology*, vol. 118, no. 2, pp. 380–389, 2000.

[7] M. Yamazaki and K. Chiba, "Genipin exhibits neurotrophic effects through a common signaling pathway in nitric oxide synthase-expressing cells," *European Journal of Pharmacology*, vol. 581, no. 3, pp. 255–261, 2008.

[8] J. Tian, Y. Cui, L. Hu et al., "Antidepressant-like effect of genipin in mice," *Neuroscience Letters*, vol. 479, no. 3, pp. 236–239, 2010.

[9] C. Yao, B. Liu, C. Chang, S. Hsu, and Y. Chen, "Preparation of networks of gelatin and genipin as degradable biomaterials," *Materials Chemistry and Physics*, vol. 83, no. 2-3, pp. 204–208, 2004.

[10] Q. S. Wang, Y. Xiang, Y. L. Cui, K. M. Lin, and X. F. Zhang, "Dietary blue pigments derived from genipin, attenuate inflammation by inhibiting LPS-induced iNOS and COX-2 expression via the NF-κB inactivation," *PLoS ONE*, vol. 7, no. 3, Article ID e34122, 2012.

[11] E. M. Merisko-Liversidge and G. G. Liversidge, "Drug nanoparticles: formulating poorly water-soluble compounds," *Toxicologic Pathology*, vol. 36, no. 1, pp. 43–48, 2008.

[12] H. Kunieda and K. Shinoda, "Krafft points, critical micelle concentrations, surface tension, and solubilizing power of aqueous solutions of fluorinated surfactants," *The Journal of Physical Chemistry*, vol. 80, no. 22, pp. 2468–2470, 1976.

[13] C. Leuner and J. Dressman, "Improving drug solubility for oral delivery using solid dispersions," *European Journal of Pharmaceutics and Biopharmaceutics*, vol. 50, no. 1, pp. 47–60, 2000.

[14] T. Vasconcelos, B. Sarmento, and P. Costa, "Solid dispersions as strategy to improve oral bioavailability of poor water soluble drugs," *Drug Discovery Today*, vol. 12, no. 23-24, pp. 1068–1075, 2007.

[15] V. Shinde, P. Amsa, S. Tamizharasi, D. Karthikeyan, T. Sivakumar, and A. Kosalge, "Nanosuspensions: a promising drug delivery strategy," *Research Journal of Pharmacy and Technology*, vol. 3, pp. 39–44, 2010.

[16] D. Mijatovic, J. Eijkel, and A. van den Berg, "Technologies for nanofluidic systems: top-down vs. bottom-up—a review," *Lab on a Chip—Miniaturisation for Chemistry and Biology*, vol. 5, no. 5, pp. 492–500, 2005.

[17] P. G. Debenedetti, J. W. Tom, X. Kwauk, and S.-D. Yeo, "Rapid expansion of supercritical solutions (RESS): fundamentals and applications," *Fluid Phase Equilibria*, vol. 82, no. 1, pp. 311–321, 1993.

[18] C. M. Keck and R. H. Müller, "Drug nanocrystals of poorly soluble drugs produced by high pressure homogenisation," *European Journal of Pharmaceutics and Biopharmaceutics*, vol. 62, no. 1, pp. 3–16, 2006.

[19] S. Schultz, G. Wagner, K. Urban, and J. Ulrich, "High-pressure homogenization as a process for emulsion formation," *Chemical Engineering & Technology*, vol. 27, no. 4, pp. 361–368, 2004.

[20] M. Pääkko, M. Ankerfors, H. Kosonen et al., "Enzymatic hydrolysis combined with mechanical shearing and high-pressure homogenization for nanoscale cellulose fibrils and strong gels," *Biomacromolecules*, vol. 8, no. 6, pp. 1934–1941, 2007.

[21] X. Zhao, K. Song, S. Wang, Y. Zu, N. Li, and X. Yu, "Micronization of the pharmaceutically active agent genipin by an antisolvent precipitation process," *Chemical Engineering & Technology*, vol. 36, no. 1, pp. 33–42, 2013.

[22] Y. Zhang, F. C. Meng, Y. L. Cui, and Y. F. Song, "Enhancing effect of hydroxypropyl-β-cyclodextrin on the intestinal absorption process of genipin," *Journal of Agricultural and Food Chemistry*, vol. 59, no. 20, pp. 10919–10926, 2011.

[23] P. G. Debenedetti, J. W. Tom, X. Kwauk, and S.-D. Yeo, "Rapid expansion of supercritical solutions (RESS): fundamentals and applications," *Pharmaceutical Research*, vol. 10, no. 3, pp. 362–368, 1993.

[24] Y. Zu, L. Meng, X. Zhao et al., "Preparation of 10-hydroxycamptothecin-loaded glycyrrhizic acid-conjugated bovine serum albumin nanoparticles for hepatocellular carcinoma-targeted drug delivery," *International Journal of Nanomedicine*, vol. 8, pp. 1207–1222, 2013.

[25] G. Thakur, A. Mitra, A. Basak, D. Rousseau, and K. Pal, "Characterization of oil-in-water gelatin emulsion gels: effect of homogenization time," in *Proceedings of the IEEE International Conference on Systems in Medicine and Biology (ICSMB '10)*, pp. 305–308, Kharagpur, India, December 2010.

[26] W. Tiyaboonchai, W. Tungpradit, and P. Plianbangchang, "Formulation and characterization of curcuminoids loaded solid lipid nanoparticles," *International Journal of Pharmaceutics*, vol. 337, no. 1-2, pp. 299–306, 2007.

[27] V. Majerik, G. Charbit, E. Badens et al., "Bioavailability enhancement of an active substance by supercritical antisolvent precipitation," *Journal of Supercritical Fluids*, vol. 40, no. 1, pp. 101–110, 2007.

[28] A. Lust, I. Laidmäe, M. Palo et al., "Solid-state dependent dissolution and oral bioavailability of piroxicam in rats," *European Journal of Pharmaceutical Sciences*, vol. 48, no. 1-2, pp. 47–54, 2012.

[29] J. Hu, W. K. Ng, Y. Dong, S. Shen, and R. B. H. Tan, "Continuous and scalable process for water-redispersible nanoformulation of poorly aqueous soluble APIs by antisolvent precipitation and spray-drying," *International Journal of Pharmaceutics*, vol. 404, no. 1-2, pp. 198–204, 2011.

[30] X. Zhao, C. Shan, Y. Zu et al., "Preparation, characterization, and evaluation in vivo of Ins-SiO_2-HP55 (insulin-loaded silica coating HP55) for oral delivery of insulin," *International Journal of Pharmaceutics*, vol. 454, no. 1, pp. 278–284, 2013.

[31] L. M. Mallis, A. B. Sarkahian, H. A. Harris, M. Y. Zhang, and O. J. McConnell, "Determination of rat oral bioavailability of soy-derived phytoestrogens using an automated on-column extraction procedure and electrospray tandem mass spectrometry," *Journal of Chromatography B: Analytical Technologies in the Biomedical and Life Sciences*, vol. 796, no. 1, pp. 71–86, 2003.

[32] K.-Y. Yang, L.-C. Lin, T.-Y. Tseng, S.-C. Wang, and T.-H. Tsai, "Oral bioavailability of curcumin in rat and the herbal analysis from *Curcuma longa* by LC-MS/MS," *Journal of Chromatography B*, vol. 853, no. 1-2, pp. 183–189, 2007.

[33] X. Cao, S. T. Gibbs, L. Fang et al., "Why is it challenging to predict intestinal drug absorption and oral bioavailability in human using rat model," *Pharmaceutical Research*, vol. 23, no. 8, pp. 1675–1686, 2006.

[34] C. Carter, T. C. Fisher, H. Hamai et al., "Haemorheological effects of a nonionic copolymer surfactant (Poloxamer 188)," *Clinical Hemorheology and Microcirculation*, vol. 12, no. 1, pp. 109–120, 1992.

[35] P. P. Constantinides, "Lipid microemulsions for improving drug dissolution and oral absorption: physical and biopharmaceutical aspects," *Pharmaceutical Research*, vol. 12, no. 11, pp. 1561–1572, 1995.

[36] J. Floury, A. Desrumaux, and J. Lardières, "Effect of high-pressure homogenization on droplet size distributions and rheological properties of model oil-in-water emulsions," *Innovative Food Science & Emerging Technologies*, vol. 1, no. 2, pp. 127–134, 2000.

[37] N. Blagden, M. de Matas, P. T. Gavan, and P. York, "Crystal engineering of active pharmaceutical ingredients to improve solubility and dissolution rates," *Advanced Drug Delivery Reviews*, vol. 59, no. 7, pp. 617–630, 2007.

[38] A. Dokoumetzidis, V. Papadopoulou, and P. Macheras, "Analysis of dissolution data using modified versions of Noyes-Whitney equation and the Weibull function," *Pharmaceutical Research*, vol. 23, no. 2, pp. 256–261, 2006.